

UCSF

UC San Francisco Previously Published Works

Title

White matter microstructural correlates of relapse in alcohol dependence

Permalink

<https://escholarship.org/uc/item/78x4v4q8>

Authors

Zou, Yukai
Murray, Donna E
Durazzo, Timothy C
et al.

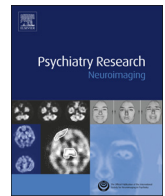
Publication Date

2018-11-01

DOI

10.1016/j.psychoresns.2018.09.004

Peer reviewed



White matter microstructural correlates of relapse in alcohol dependence

Yukai Zou^{a,b}, Donna E. Murray^{c,d}, Timothy C. Durazzo^{e,f}, Thomas P. Schmidt^c, Troy A. Murray^c, Dieter J. Meyerhoff^{c,d,*}

^a Weldon School of Biomedical Engineering, Purdue University, West Lafayette, IN 47906, United States

^b College of Veterinary Medicine, Purdue University, West Lafayette, IN 47906, United States

^c Center for Imaging of Neurodegenerative Diseases (CIND), San Francisco VA Medical Center, San Francisco, CA 94121, United States

^d Department of Radiology and Biomedical Imaging, University of California San Francisco, San Francisco, CA 94143, United States

^e Department of Psychiatry and Behavioral Sciences, Stanford University School of Medicine, Stanford, CA 94305, United States

^f Mental Illness Research Mental Illness Research and Education Clinical Centers, Sierra-Pacific War Related Illness and Injury Study Center, VA Palo Alto Health Care System, Palo Alto, CA 94304, United States

ARTICLE INFO

Keywords:

Diffusion tensor imaging
White matter
Alcohol use disorder
Relapse risk
Abstinence
Smoking

ABSTRACT

Identification of neural correlates of relapse to alcohol after treatment is clinically important as it may inform better substance abuse treatment. Few studies have specifically analyzed the white matter microstructure in treatment seekers as it might relate to relapse risk versus long-term abstinence. Using 4 Tesla diffusion tensor imaging, we compared two groups of one-month-abstinent treatment-seekers, who were classified based on their drinking status between six and nine months after treatment initiation. We hypothesized that subsequent relapsers had greater white matter microstructural deficits in specific brain regions than long-term abstainers. At one month of abstinence, 37 future relapsers versus 25 future abstainers had lower fractional anisotropy (a measure of axonal organization and membrane integrity) in the corpus callosum and right stria terminalis/fornix, higher diffusivity in the genu of the corpus callosum, left and right stria terminalis/fornix, and lower diffusivity in left anterior corona radiata. These differences existed despite similar lifetime and recent drinking and smoking histories in the groups. Longer smoking duration in relapsers was associated with lower fractional anisotropy in right stria terminalis/fornix. The study identified specific microstructural biomarkers of alcohol relapse risk in adults, contributing to the definition of a neurobiological relapse risk profile in alcohol use disorder.

1. Introduction

Alcohol use disorder (AUD) is associated with a chronically relapsing-remitting course over lifetime (Witkiewitz and Marlatt, 2007). Most individuals treated for AUD will relapse to hazardous alcohol consumption within just six months of treatment (Kirshenbaum et al., 2009; Meyerhoff and Durazzo, 2010; Witkiewitz, 2011). Resumption to hazardous drinking for long periods relates to clinically significant impairments of psychosocial functioning (e.g., unemployment, relationship/marital discord, legal entanglements) and maintains cognitive dysfunction in AUD (Durazzo et al., 2008; Maisto et al., 2006, 2007). On the other hand, sustained abstinence following treatment relates to significant improvements in neurocognitive and adaptive psychosocial functioning (e.g., Pennington et al., 2013 and references cited therein) and to at least partial recovery from prefrontal

neurobiological injury thought to be related to previous chronic heavy alcohol use (for reviews see Buhler and Mann, 2011; Xiao et al., 2015; Zahr, 2014).

Various neuroimaging modalities have been employed to characterize brain changes with chronic alcohol consumption and to identify potential imaging biomarkers of increased relapse risk after AUD treatment (e.g., Meyerhoff and Durazzo, 2010; Meyerhoff et al., 2013; Seo and Sinha, 2014, 2015; for review see Moeller and Paulus, 2018). Brain biomarkers measured either alone or together with other markers often provide better predictions of treatment outcomes than measures of for example education, neurocognition, craving, stress or psychiatric symptomatology (e.g., Volkow and Baler, 2013; Gabrieli et al., 2015). Identification of specific neural correlates of relapse are therefore clinically important as it may inform better substance abuse treatment and predict long-term clinical outcomes. For example, structural

* Corresponding author at: Center for Imaging of Neurodegenerative Diseases (CIND), San Francisco VA Medical Center, 4150 Clement Street (114M), San Francisco, CA 94121, United States.

E-mail address: dieter.meyerhoff@ucsf.edu (D.J. Meyerhoff).

<https://doi.org/10.1016/j.pychresns.2018.09.004>

Received 25 December 2017; Received in revised form 14 September 2018; Accepted 14 September 2018

Available online 18 September 2018

0925-4927/ © 2018 Elsevier B.V. All rights reserved.

magnetic resonance imaging (MRI) performed at treatment entry showed that alcohol dependent individuals who relapsed after treatment have less cortical gray matter than those who sustained several months of abstinence, in particular in prefrontal regions including the orbitofrontal, anterior cingulate, and dorsolateral prefrontal cortices (Beck et al., 2012; Cardenas et al., 2011; Durazzo et al., 2011; Rando et al., 2011; Seo et al., 2015). An early study also reported reduced amygdala volume in future relapsers versus abstainers and generally smaller hippocampi compared to healthy controls (Wrase et al., 2008). The structural integrity of these brain regions and the neural networks they are embedded in are critically important for impulse/inhibitory control, emotional regulation, craving, and evaluation/anticipation of stimulus salience and hedonics, concepts important for the development and persistence of addictive disorders including relapse (Koob and Volkow, 2016; Volkow and Baler, 2013; Volkow et al., 2012).

Diffusion tensor imaging (DTI) is another modality to probe in-vivo brain morphology in AUD. It is based on the differential diffusivity of water molecules along or perpendicular to white matter tracts and provides measures of local white matter microstructural integrity that complement macrostructural measurements of cortical and white matter volumes. One DTI metric commonly computed is fractional anisotropy (FA), a sensitive marker of white matter organization or fiber coherence at the microstructural level, reflecting axonal organization and membrane integrity. White matter FA has been generally found to be lower in corpus callosum, major frontocortico-striatal tracts and limbic pathways of individuals with AUD compared to healthy controls (Yeh et al., 2008; Gazdzinski et al., 2010; Kuceyeski et al., 2013; Monnig et al., 2015; Sorg et al., 2015; Zou et al., 2017). Lower FA in AUD is interpreted to reflect primarily axonal dystrophy or loss and demyelination or myelin loss (Beaulieu, 2002; Zahr, 2014), which is also associated with natural processes of white matter aging (Peters, 2002). Although FA deficits have been described in long-term alcohol abstinent individuals (Fortier et al., 2014), lower regional FA also has been shown to be at least partly reversible over short (Gazdzinski et al., 2010; Zou et al., 2017) and longer periods of abstinence from alcohol (Pfefferbaum et al., 2014).

Few studies to date, however, have specifically analyzed the white matter microstructure as it might relate to relapse risk versus successful long-term abstinence from chronic heavy drinking: One study (Sorg et al., 2012) showed significantly lower FA in major fiber tracts of the anterior brain including corpus callosum and forceps minor of 16 treatment seeking alcoholics at 3 weeks of abstinence who had resumed heavy drinking within 6 months, compared to 29 matched alcoholics who largely maintained abstinence over that same period. Another smaller study demonstrated only statistically weak regional FA reductions in the corpus callosum and fornix at 1 year of abstinence in 10 individuals who relapsed to heavy drinking within the subsequent years compared to those 27 who managed to abstain over the same time (Pfefferbaum et al., 2014). In treatment-seeking adolescents, who had not been exposed to chronic alcohol consumption for long, lower FA in prefrontal brain and temporal lobe was related to greater alcohol problem severity (drinking frequency) at 6-month follow-up (Chung et al., 2013). Given the dearth of information on these potential microstructural biomarkers of relapse risk in treatment-seeking adults and the relatively small numbers of resusers/relapsers in these studies, we compared treatment-seekers at one month of abstinence, who were classified based on their drinking status (abstinent or relapsed) between 6 and 9 months after treatment initiation. We hypothesized that high-resolution DTI data obtained at about one month of abstinence show that subsequent relapsers (REL) had greater regional white matter microstructural deficits than long-term abstainers (ABST). Our analyses focused on the participants we previously found to have deficits in white matter integrity compared to light/non-drinking controls (Zou et al., 2017), on those white matter tracts that we and others found affected by chronic alcohol consumption and relapse status, and on the potential effects of chronic cigarette smoking on our primary DTI

measures. The presented analyses expand a growing body of literature on the definition of a neurobiological relapse risk profile for AUD, which may be employed clinically to focus treatment resources on those most in need.

2. Methods

2.1. Participants

Sixty-two alcohol dependent individuals were recruited from the VA Medical Center Substance Abuse Day Hospital and the Kaiser Permanente Chemical Dependence Recovery outpatient treatment clinics in San Francisco; all were in treatment and verifiably abstinent for approximately 1 month when structural neuroimaging was performed. The predominantly male Veteran participants were between 25 and 70 years of age and all met DSM-IV criteria for alcohol dependence. Forty-three participants from our previous account of this population (Zou et al., 2017) were included in the current study. All participants provided written informed consent prior to study procedures that had been approved by the University of California San Francisco and the VA Medical Center in accordance with the Declaration of Helsinki.

Inclusion/exclusion criteria: Primary inclusion criteria were fluency in English, DSM-IV diagnosis of alcohol dependence or abuse at baseline (all met criteria for alcohol dependence), consumption of > 150 standard alcohol-containing drinks (i.e., 13.6 grams of pure ethanol) per month for > 8 years prior to enrollment for males, and > 80 drinks per month for > 6 years prior to enrollment for females. Exclusion criteria were a history of the following: dependence on any substance other than alcohol or nicotine in the 5 years immediately prior to enrollment, any intravenous drug use in the 5 years prior to baseline study, opioid agonist/replacement therapy, intrinsic cerebral masses, HIV/AIDS, cerebrovascular accident, cerebral aneurysm, arteriovenous malformations, myocardial infarction, medically uncontrolled chronic hypertension, type-I diabetes, chronic obstructive pulmonary disease, non-alcohol related seizures, significant exposure to established neurotoxins, demyelinating and neurodegenerative diseases, Wernicke-Korsakoff syndrome, delirium, penetrating head injury, and closed head injury resulting in loss of consciousness > 10 minutes. Psychiatric exclusion criteria were history of schizophrenia-spectrum disorders, bipolar disorder, cyclothymia, PTSD, obsessive-compulsive disorder and panic disorder. Not exclusionary were hepatitis C (by self-report and medical charts review), type-2 diabetes, hypertension, unipolar mood disorders (i.e., major depression, substance-induced mood disorder), given their high prevalence in those with an AUD (Grant et al., 2015; Mertens et al., 2005). Participants seropositive for hepatitis C did not take interferon or other medications to manage active symptomatology. Participants were breathalyzed and urine-tested for illicit substances before assessment and no participant tested positive for any tested substances at any assessment.

2.2. Clinical Measures

At baseline, participants completed the Clinical Interview for DSM-IV Axis I Disorders, Version 2.0 (SCID-I/P) and semi-structured interviews for lifetime alcohol consumption (Lifetime Drinking History) and substance use (in-house questionnaire assessing substance type, and quantity and frequency of use) (Pennington et al., 2013). From the Lifetime Drinking History, average number of alcoholic drinks/month over 1 year prior to enrollment and average number of drinks/month over lifetime were calculated. All participants also completed standardized questionnaires assessing impulsivity (Barratt Impulsivity Scale, BIS-11) (Patton et al., 1995), depressive (Beck Depression Inventory, BDI) (Beck, 1978) and anxiety symptomatology (State-Trait Anxiety Inventory, Trait form Y-2, STAI) (Spielberger et al., 1977), as well as nicotine dependence (Fagerström Tolerance Test for Nicotine Dependence, FTND) (Heatherton et al., 1991). As white matter microstructure

Table 1

Demographic, clinical, medical and psychiatric measures in ABST and REL reported in mean \pm standard deviation for the entire groups and subsample of female participants (in parentheses). BDI: Beck Depression Inventory; BIS: Barratt Impulsiveness Scale; FTND: Fagerstrom Test for Nicotine Dependence; STAI: Spielberger State Trait Anxiety Index. NS: not significant.

	ABST (females)	REL (females)	Group comparisons
n	25 (6)	37 (3)	
Duration of Abstinence [days]	32.8 \pm 8.7 (33.2 \pm 6.4)	30.2 \pm 9.9 (24.7 \pm 17.4)	NS
Age [years]	52.1 \pm 12.2 (59.7 \pm 6.5)	49.7 \pm 9.3 (57.7 \pm 4.0)	NS
1-year average drinks/month*	380 \pm 200 (300 \pm 131)	371 \pm 235 (198 \pm 68)	NS
Lifetime average drinks/month*	190 \pm 97 (178 \pm 121)	212 \pm 133 (87 \pm 27)	NS
Comorbid psychiatric disorder [n]	7 (2)	16 (1)	NS
Comorbid medical condition [n]	15 (3)	27 (3)	NS
Comorbid substance-use disorder [n]	7 (3)	14 (0)	NS
Number of smokers [n]	14 (2)	25 (1)	NS
FTND total	2.5 \pm 2.6 (1.5 \pm 2.5)	2.5 \pm 2.1 (1.5 \pm 1.7)	NS
Cigarettes/day	9 \pm 10 (5 \pm 8)	8 \pm 8 (1 \pm 2)	NS
Years of smoking at current level	12.8 \pm 14.7 (8.3 \pm 14.4)	10.2 \pm 12.9 (0.3 \pm 0.6)	NS
Total lifetime years of smoking	16.9 \pm 16.9 (10.7 \pm 16.7)	19.0 \pm 16.4 (1.3 \pm 2.3)	NS
BDI	11.8 \pm 8.2 (7.8 \pm 8.1)	10.8 \pm 7.2 (4.0 \pm 2.6)	NS
BIS-11 total	64.5 \pm 8.9 (70.6 \pm 6.5)	64.8 \pm 10.6 (62.0 \pm 2.0)	NS
BIS-11 - attention	16.5 \pm 3.2 (19.6 \pm 1.7)	15.7 \pm 4.0 (13.7 \pm 2.5)	NS
BIS-11 - motor	23.0 \pm 3.3 (24.6 \pm 2.6)	22.5 \pm 4.7 (23.7 \pm 1.5)	NS
BIS-11 - non-planning	25.0 \pm 5.4 (26.4 \pm 5.9)	26.5 \pm 4.6 (24.7 \pm 2.31)	NS
STAI - state	33.8 \pm 12.1 (32.3 \pm 12.8)	35.6 \pm 9.8 (24.7 \pm 5.0)	NS
STAI - trait	42.4 \pm 9.9 (42.3 \pm 11.0)	44.7 \pm 10.5 (35.3 \pm 4.5)	NS
Processing speed domain [z-score]	-0.1 \pm 0.6 (0.3 \pm 0.5)	-0.2 \pm 0.6 (-0.6 \pm 0.5)	NS

*1 alcoholic drink contains 13.6 g of ethanol.

was shown to correlate with processing speed (Sorg et al., 2015), we also measured processing speed (composite z-scores for Trail Making Test A and B) (Reitan and Wolfson, 1985) and WAIS Digit Symbol encoding (Wechsler, 1997) at the time of neuroimaging. Basic demographics, substance use and behavioral measures are summarized in Table 1.

2.3. MR data acquisition

A 4T Bruker MedSpec system with Siemens Trio console was used for acquiring MR images (Siemens, Erlangen, Germany). A 3D sagittal magnetization prepared rapid gradient echo sequence was used to acquire T1 data (TR/TE/TI = 2300/3/950 ms, $1 \times 1 \times 1 \text{ mm}^3$), and a 2D axial turbo-spin echo sequence acquired T2 data (TR/TE = 8400/70 ms, $0.9 \times 0.9 \times 3 \text{ mm}^3$). A dual spin echo planar imaging sequence was used to acquire 40 3-mm-thick interleaved slices (no gap) of the diffusion-weighted data (TR/TE = 6000/77 ms, $2 \times 2 \text{ mm}^2$ in-plane), using six diffusion-encoding directions at $b = 800 \text{ s/mm}^2$ and one at $b = 0 \text{ s/mm}^2$. To reduce geometrical distortions, twofold parallel imaging acceleration was applied. Four scans were averaged after acquisition to boost signal-to-noise. Further details of data acquisition have been reported (Kuceyeski et al., 2013; Zou et al., 2017).

2.4. DTI data processing

2.4.1. Pre-processing

Data were processed as previously described (Zou et al., 2017). In short, T1- and T2-weighted structural images were processed using an expectation maximization segmentation algorithm (Van Leemput et al., 1999a, b) that included bias correction and skull stripping for T1 and resampling and reslicing for T2 images. The diffusion-weighted data were processed through an in-house python-based pipeline (TEEM), where the DTI data was up-scaled to the processed T1 image resolution, and the processed T2 image was registered to the $b = 0$ image for geometric distortion correction. A $b = 0$ mask was automatically generated by TEEM, and any distortions or inaccuracies were manually corrected. After masking, the $b = 0$ image was then registered to the processed T1 image. The eigenvectors, diffusion tensor, mean diffusivity (MD), and FA for each voxel were computed, and quality controls confirmed accuracy for each final FA map. Only cases satisfying all

quality control criteria (Zou et al., 2017) were included in the subsequent Tract-Based Spatial Statistics (TBSS) analyses, with the most common problems being registration issues between the T2 mask and the T1 or $b = 0$ images. Seven ABST and 3 REL failed these quality control criteria and were therefore excluded, which resulted in a total of 62 subjects for the final analyses.

2.4.2. Tract-based spatial statistics (TBSS)

All FA maps were processed via FSL's TBSS (Smith et al., 2006) for voxel-wise group-level analysis. First, individual images were aligned through a nonlinear transformation algorithm to FSL's FMRIB58 FA template that contains 58 high-resolution FA data sets from healthy male and female subjects aged 20–50 years. Next, all warped FA images were normalized to the Montreal Neurological Institute standard space (MNI152 T1, 1 mm spatial resolution). A mean FA image was created from all data in the datasets and thinned to generate a mean FA skeleton that represents the locally maximal FA values. The mean FA skeleton was thresholded at $FA > 0.20$ to reduce partial volume effects between the borders of different tissues, yielding a subject-specific skeleton. The partial volume effects were further reduced by projecting the regional maximal FA values onto the skeleton according to a distance map (Smith et al., 2006). Mean diffusivity was normalized to the skeleton using procedures also described on the FSL site for non-FA images.

2.5. Definition of abstainers and relapsers

2.5.1. Abstainers

Participants were designated Abstainers (ABST, $n = 25$) if they met all the following criteria: a) self-report (in-person or via telephone interview) of no alcohol consumption between treatment entry and follow-up assessments 6 to 9 months after treatment entry; b) no report of alcohol consumption between treatment entry and follow-up assessments in available medical records; and c) our laboratory indicators of alcohol consumption (here γ -glutamyl-transferase) obtained in more than 80% of the participants at follow-up were within normal limits.

2.5.2. Relapsers

Participants were designated Relapsers (REL, $n = 37$) if they met any of the following conservative criteria: a) self-report (in-person or

via telephone interview) of any alcohol consumption between 1 and 9 months after treatment entry at follow-up assessments 6–9 months after treatment entry; b) any alcohol consumption or relapse between treatment entry and follow-up assessment as indicated in medical records; and c) any alcohol use by a participant reported by telephone by a relative or close friend of the participant. In our previous studies, any level of alcohol consumption following treatment was associated with poorer psychosocial functioning (Durazzo et al., 2008).

2.6. Statistical analyses

2.6.1. Demographic, clinical, medical and psychiatric variables

ABST and REL were compared on baseline demographics, substance use data, and proportions of comorbid medical, psychiatric, and substance use disorders. Group comparisons were conducted with independent sample *t*-tests or Fisher's Exact Test when indicated, and $p < 0.05$ was considered statistically significant.

2.6.2. Region-of-interest (ROI) analysis

The mean FA and MD skeletons from the TBSS analyses were fed into voxel-wise permutation-based cross-subject statistics. Within each *a priori* ROI and its contralateral region, voxel-wise statistics between the two groups (ABST vs. REL) were conducted with 5000 permutations using the FSL *Randomise* program (v2.9, <http://fsl.fmrib.ox.ac.uk/fsl/fslwiki/Randomise>) with threshold-free cluster enhancement to control type I error (Nichols and Holmes, 2002). We restricted our comparisons of ABST and REL to ROIs we had previously shown to differentiate alcohol-dependent individuals and controls (Zou et al., 2017) and that were shown by others to be affected in AUD individuals (Monnig et al., 2015; Pfefferbaum et al., 2014; Sorg et al., 2015; Sorg et al., 2012). The *a priori* ROIs were: corpus callosum, bilateral anterior corona radiata, bilateral forceps minor, right superior corona radiata, right cingulum, right hippocampus, bilateral internal and external capsules, left superior fronto-occipital fasciculus, and fornix; they are displayed in Fig. 1. Our primary analyses used voxel-wise statistics between the two groups for each of these *a priori* ROIs. In secondary analyses, we ran the same voxel-wise statistics on the contralateral regions of any unilateral *a priori* ROI. We also ran exploratory TBSS analysis for regions outside of the *a priori* ROIs with the same statistics. After the two-group voxel-wise statistics, the clusters within the *a priori* ROIs underwent additional family-wise error (FWE) corrections across space for the size of the skeleton in the ROI, and the largest significant ($p < 0.05$ corrected) cluster within each ROI was selected for extracting FA and MD values with the FSL cluster program. The corresponding fiber tracts of the

clusters were identified on the Johns Hopkins white matter label atlas (JHU-ICBM-DTI-81 and JHU-ICBM-tracts-maxprob-thr50-1 mm, <http://cmrm.med.jhmi.edu/>) (Mori et al., 2005).

To assess for group differences in our regional FA and MD measures, an abstinence status (REL or ABST) \times smoking status (smoker or non-smoker) analysis of covariance (ANCOVA) was performed using as covariates age, average monthly drinks in last year, and/or presence of comorbidities (psychiatric disorder, substance-use disorder, or medical condition). These covariates (except age) have been shown to be associated with group membership and/or duration of abstinence following treatment for AUD (Durazzo et al., 2008; Durazzo et al., 2011; Pfefferbaum et al., 2004; Weinberger et al., 2015). The corresponding *p*-values for any significant main effect and interaction were FDR corrected for the number of *a priori* ROIs (adjusted $p = 0.028$). The exploratory TBSS analyses used $p < 0.01$ to mitigate against type-I errors.

To investigate associations between cluster-specific DTI metrics and measures of behavior (impulsivity, depressive and anxiety symptoms), substance use, and processing speed, Pearson's partial correlations were computed with age as covariate; the findings were controlled for multiple comparisons using FWE (corrected $p = 0.05/6 = 0.008$. We used R 3.2.0 for all statistical analyses (R Foundation for Statistical Computing, 2012).

3. Results

3.1. Demographic, substance use, behavioral, and cognitive outcome measures

The ABST and REL groups were statistically equivalent on age, duration of abstinence from alcohol at time of study, and several lifetime drinking and smoking measures. The groups also did not differ on self-reported impulsivity scores, mood measures, and the cognitive domain of processing speed. While the REL group had numerically more individuals with comorbid cigarette smoking, medical conditions, substance and other psychiatric disorders, none of these proportional differences approached statistical significance (all $p > 0.28$) (see Table 1; values in parentheses are for the few female participants included). Specifically, 5 ABST and 9 REL were comorbid for cocaine use disorder, 2 and 8 comorbid for marijuana use disorder, 2 and 2 comorbid for methamphetamine use disorder, 1 and 5 comorbid for opioids, and 1 REL each abused valium and LSD. Three ABST and 4 REL had hepatitis C, 10 and 11 had medically-controlled hypertension, and 3 and 5 had high cholesterol. Further, while 6 ABST and 7 REL had current major depressive disorder, 2 and 1 had panic/anxiety disorder,

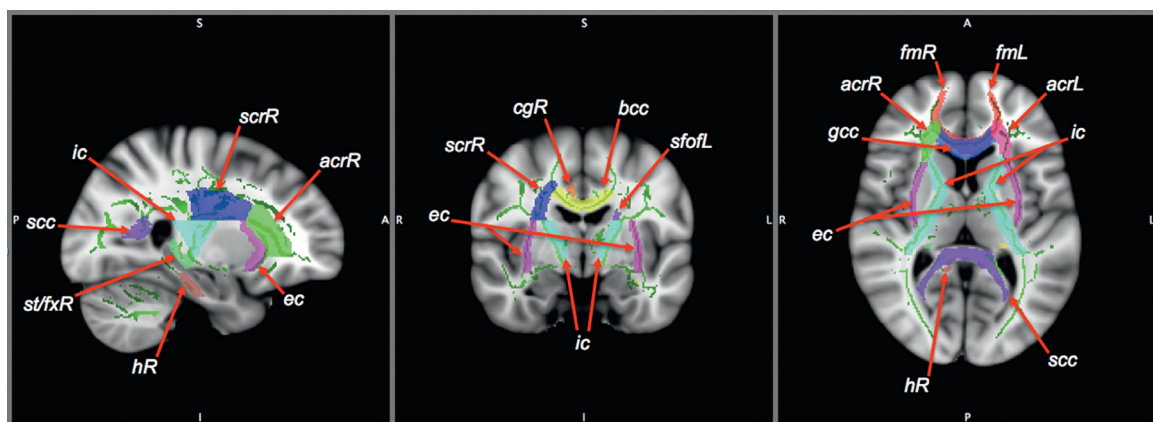


Fig. 1. *A priori* regions of interest (ROIs), overlaid on the skeleton (green) derived from tract-based spatial statistics, and on the MNI template ($1.0 \times 1.0 \times 1.0 \text{ mm}^3$) in sagittal, coronal, and axial views. The ROIs are corpus callosum (bcc: body; gcc: genu; scc: splenium), anterior corona radiata (acr), forceps minor (fm), right superior corona radiata (scrR), right cingulum (cgR), right hippocampus (hR), internal (ic) and external (ec) capsules, left superior fronto-occipital fasciculus (sfofL), and stria terminalis/fornix (st/fx). L/R: left/right hemisphere. (For interpretation of the references to color in this figure legend, the reader is referred to the web version of this article.)

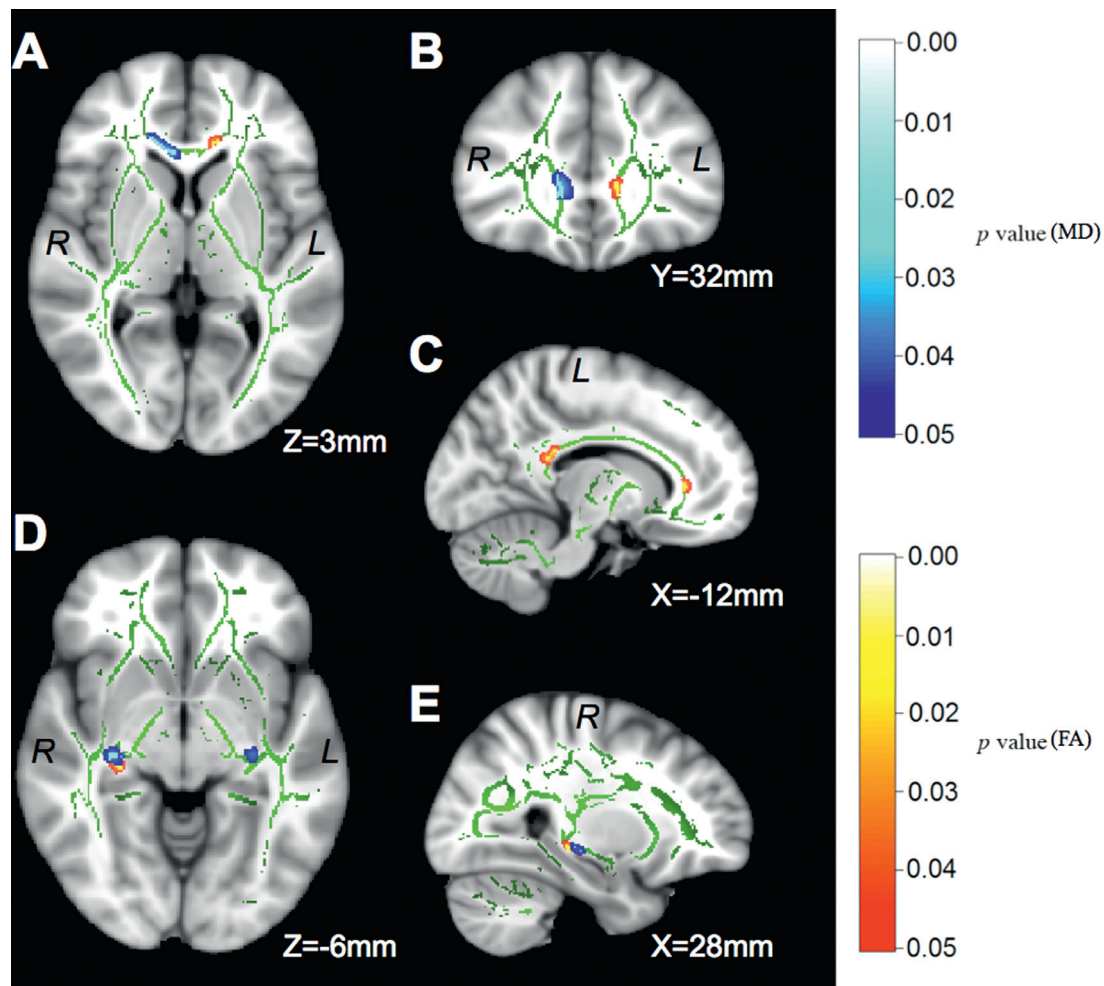


Fig. 2. *t*-statistical maps of TBSS analyses showing the DTI differences between ABST and REL at 1 month of abstinence. The TBSS skeleton (green) is overlaid on the MNI template ($1 \times 1 \times 1 \text{ mm}^3$) and displayed in sagittal, coronal, and axial views. The metric in the bottom-right corner indicates the distance from the anterior commissure. All significant clusters are FWE corrected ($p < 0.05$). FA (red-yellow) is higher in ABST than REL in the genu (A and C) and splenium (C) of the corpus callosum, and the right stria terminalis (D and E). MD (blue-light blue) is higher in REL than ABST in the genu of the corpus callosum (A and B), the left (D) and right (D and E) stria terminalis. A cluster of lower MD in the left anterior corona radiata of REL versus ABST is not shown. See Table 2 for the corresponding statistics of each cluster. R/L: right/left hemisphere. (For interpretation of the references to color in this figure legend, the reader is referred to the web version of this article.)

and 3 REL had a positive tuberculosis skin test.

3.2. Relapsers (REL) vs. Abstainers (ABST)

3.2.1. Fractional anisotropy (FA)

The interaction between abstinence status and smoking status was not significant for any of the *a priori* ROIs. There were main effects of abstinence status in the left parts of the genu and splenium of the corpus callosum (genu: size = 31 mm^3 , $F[1,56] = 20.40$, $p < 0.001$, corrected for age, drinking severity, and comorbid medical condition, Fig. 2A, B, C; splenium: size = 38 mm^3 , $F[1,60] = 12.95$, $p < 0.001$, no significant covariates, Fig. 2C) and a cluster of 41 mm^3 in the right stria terminalis/fornix ($F[1,60] = 11.77$, $p = 0.001$, no significant covariates, Fig. 2D, E), with lower FA values in REL than ABST (Table 2). No regions showed higher FA in REL. There was no significant main effect of smoking status, and neither comorbid psychiatric conditions nor comorbid substance-use disorder diagnoses were significant covariates. Re-analyzing the data without the few female participants included (6 in ABST, 3 in REL) did not yield findings that differed significantly from our main analyses reported above. Secondary TBSS analyses showed no statistically significant cluster within the contralateral regions of any unilateral *a priori* ROI. An exploratory whole-brain TBSS analysis revealed a single cluster of 89 mm^3 size in the cerebral peduncle (FA

lower in REL than ABST, $p < 0.05$ uncorrected) that was outside of our *a priori* ROIs.

3.2.2. Mean Diffusivity (MD)

Similar to FA, MD measures showed no significant interactions between abstinence status and smoking status in any of the *a priori* ROIs. Main effects of abstinence were found in a cluster of 131 mm^3 in the right part of the genu of the corpus callosum (also labeled as right forceps minor in one of the Johns Hopkins atlases) and small clusters in the right and left stria terminalis/fornix (all clusters showed MD higher in REL than ABST, all $F[1,60] > 7.15$, all $p < 0.009$, no significant covariates, Fig. 2D, E). A single cluster of 134 mm^3 in the left anterior corona radiata ($F[1,60] = 7.18$, $p = 0.009$, no significant covariates) showed lower MD in REL than ABST (Table 2). There were no significant main effects of smoking status and none of the covariates tested contributed significantly to any of the regional MD differences. Again, results without the few female individuals included did not differ significantly from those of the main MD analyses, and our secondary analyses showed no statistically significant cluster within the contralateral regions of any unilateral *a priori* ROI. Exploratory whole-brain TBSS analyses revealed a cluster of 84 mm^3 size in the right posterior thalamic radiation and a cluster of 19 mm^3 in the right tapetum (MD lower in REL than ABST, both $p < 0.05$ uncorrected) that were outside

Table 2

Regional FA and MD ($\times 10^{-3}$, mean \pm standard deviation) in 25 ABST and 37 REL at 1 month of abstinence based on the largest significant ($p < 0.05$) clusters from the two-group voxel-wise statistics, using FWE for multiple comparison correction. L/R: left/right hemisphere. Effect size was calculated using Cohen's d . # Adjusted mean \pm standard deviation with age and average monthly drinks in last year as significant covariates at $p < 0.05$. Cluster size, the peak p -value (FWE corrected), and its corresponding MNI coordinates in the cluster are reported.

Tract name	Overall F	p	ABST	REL	Effect Size	Voxels (mm^3)	p -Max	p -MAX X (mm)	p -MAX Y (mm)	p -MAX Z (mm)
FA										
Corpus callosum - genu#	$F[4,56] = 14.94$	<0.001	0.99 ± 0.17	0.92 ± 0.19	0.39	31	0.962	-12	33	4
Corpus callosum - splenium	$F[1,60] = 12.95$	<0.001	0.94 ± 0.03	0.91 ± 0.03	1.00	38	0.955	-11	-36	23
Stria terminalis R	$F[1,60] = 11.77$	0.001	0.71 ± 0.06	0.66 ± 0.06	0.83	41	0.997	30	-24	-7
MD										
Anterior corona radiata L	$F[1,60] = 7.18$	0.009	1.28 ± 0.52	0.92 ± 0.52	0.69	134	0.988	-18	30	19
Corpus callosum - genu	$F[1,60] = 8.50$	0.005	1.14 ± 0.82	1.76 ± 0.82	0.76	131	0.967	8	28	1
Stria terminalis L	$F[1,60] = 7.86$	0.007	0.91 ± 0.23	1.15 ± 0.34	0.71	13	0.967	-28	-20	-8
Stria terminalis R	$F[1,60] = 7.20$	0.009	0.89 ± 0.25	1.06 ± 0.25	0.68	36	0.983	28	-20	-7

of our *a priori* ROIs.

3.3. Associations of DTI metrics with behavioral outcome measures

In 25 smoking REL, lower FA in the right stria terminalis/fornix correlated with more years of smoking at current level ($r = -0.513$, $p = 0.010$, Fig. 3A); no such correlation was found in 14 smoking ABST ($r = 0.130$, $p = 0.672$), giving rise to a weak but non-significant correlation in the combined group ($r = -0.222$, $p = 0.181$). We did not detect—as previously reported (Sorg et al., 2015)—a significant correlation between higher FA in the genu of the corpus callosum cluster and higher processing speed z-scores of the combined AUD group ($r = 0.172$, $p = 0.194$, $n = 60$). However, when looking at this

correlation separately by group, it was significant in the ABST ($r = 0.552$, $p = 0.008$, $n = 23$; Fig. 3B) but not in the REL group ($r = 0.141$, $p = 0.413$, $n = 37$). Finally, no other significant associations were observed of any regional FA and MD measures with substance use and mood measures in any group (separate or combined).

4. Discussion

Our analyses reveal regionally specific microstructural abnormalities in the brain of treatment-seeking individuals with AUD that are associated with greater risk for resumption of hazardous drinking after treatment, validating previous such claims (Sorg et al., 2012). The microstructural findings described in this report are consistent with our previous macrostructural MR studies, in which future REL showed different types of morphological abnormalities (volume, cortical thickness) compared to ABST (see Introduction). Specifically, in this DTI study we found: (1) at 1 month of abstinence, 37 future REL exhibited lower FA and mostly higher MD than 25 future ABST in corpus callosum, frontal white matter tracts, and stria terminalis/fornix, differences that existed despite similar lifetime and recent drinking and smoking histories in the groups; and 2) longer smoking duration in REL was associated with lower FA in right stria terminalis/fornix. Although the specific brain regions that distinguish ABST and REL in this analysis have been implicated in previous studies on microstructural deficits in AUD, they are different from those that differentiated a smaller group of the same treatment seekers from non/light-drinking healthy controls (Zou et al., 2017). This suggests that alcohol dependence and relapse propensity may not necessarily be governed by the same neural mechanisms and that ways of preventing the development of AUD may not necessarily be equally successful for the prevention of relapse.

Our findings of abnormal DTI metrics in corpus callosum (both genu and splenium), frontal white matter tracts, and temporal structures of future REL compared to ABST are largely consistent with and thus validate previous literature. Chung et al. described lower FA in prefrontal brain and temporal lobe of treatment-seeking adolescents related to higher alcohol drinking frequency at 6-month-follow-up (Chung et al., 2013). Sorg et al. reported lower FA in the anterior corpus callosum and forceps minor in addition to FA deficits in superior corona radiata (where we also found MD increases in REL), anterior internal capsule, and uncinate fasciculus in 16 relapsers compared to 29 matched abstainers (Sorg et al., 2012). Pfefferbaum et al. demonstrated statistically weak regional FA differences in the corpus callosum and fornix at 1 year of abstinence between 10 individuals who relapsed to heavy drinking within the subsequent years compared to 27 treatment-seekers who managed to abstain over the same time (Pfefferbaum et al., 2014). This group also showed that relapsers have greater age-related regional FA declines than long-term abstainers, which may make the brain in older treatment seekers more vulnerable to relapse eventually. As the microstructure of the fornix and the genu of the corpus callosum is the earliest to degenerate over the lifespan (Lebel et al., 2012), these

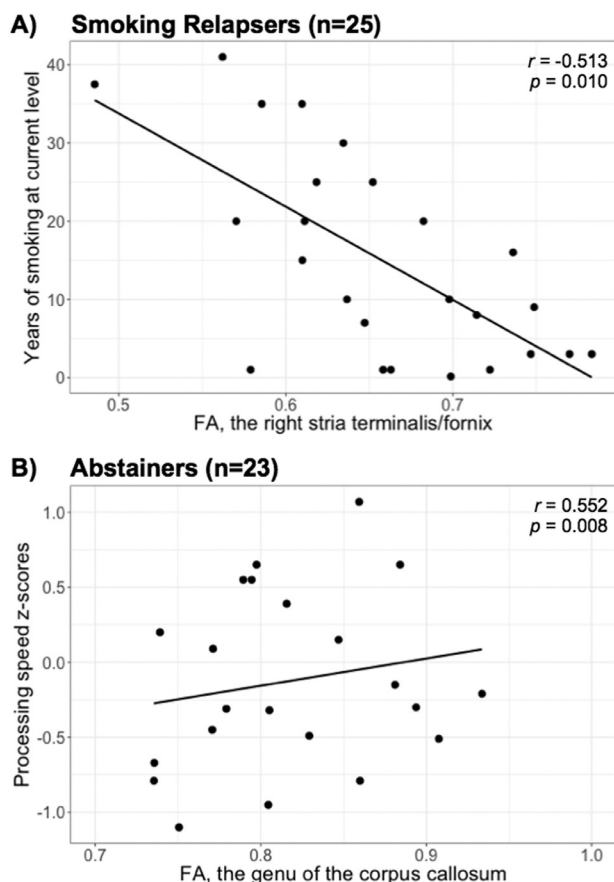


Fig. 3. Associations between (A) smoking severity (y-axis) and FA in 25 smoking relapsers, and (B) processing speed z-scores (y-axis) and FA in the genu of the corpus callosum of 23 abstainers with available data. The Pearson's correlation coefficients r are age adjusted.

chronic alcohol effects in relapsers were described as accelerated aging (Pfefferbaum et al., 2014). While our study design is akin to previous work (Sorg et al., 2012) and our results also implicate frontal white matter microstructure in relapse risk, we included a larger relapse group, followed up with our patients over a longer time after treatment initiation, used a more stringent definition of abstinence, employed theoretically more sensitive high-field instrumentation and higher DTI spatial resolution, and identified chronic smoking as a previously unappreciated and modifiable behavior that contributes to localized and behaviorally-relevant microstructural differences between future relapsers and abstainers.

The genu of the corpus callosum connects the bilateral prefrontal lobes and projects via frontal fiber bundles (including forceps minor, anterior corona radiata) to prefrontal cortical regions. These are typically shown atrophied in many neuroimaging studies of AUD (e.g., Buhler and Mann, 2011; Xiao et al., 2015). In the elderly, lower FA in the genu of the corpus callosum is associated with lower perceptual speed and longer episodic retrieval reaction time (Bucur et al., 2008; Schulte et al., 2005) as well as poor performance in reasoning (Monge et al., 2016). Furthermore, microstructural deficits in the corpus callosum and adjacent frontal white matter tracts have implications for interhemispheric communication and executive control, including inhibition, planning, initiation and maintenance of a task set (Chung et al., 2013 and references cited therein), functions that are important for the maintenance of abstinence. Correspondingly, higher FA in the genu of the corpus callosum was associated with better processing speed in our ABST but not in our REL group. Unexpectedly, REL had a large cluster of lower MD than ABST in the left anterior corona radiata, which is part of the corticopontine tract that links the frontal cortex through the internal capsule to the brainstem. Lower MD suggests higher white matter connectivity in this area of REL versus ABST, reminiscent of stronger frontostriatal resting state connectivity in AUD versus non-drinking controls and linked to deficient cognitive and emotional processing in AUD (e.g., Mueller-Oehring et al., 2015). These regional microstructural alterations may reflect (potentially compensatory) processes that contribute to an altered organization of neural circuitry to satisfy greater demands of cognitive and emotional processes associated with maintaining abstinence. Taken together, these human studies are consistent with animal research demonstrating chronic alcohol-induced myelin damage to fibers in the frontal lobe. In a rat model of alcohol consumption (Vargas et al., 2014), the investigators found a reduced cross-sectional area of the forceps minor in adult rats, which was not associated with baseline alcohol intake but with subsequent relapse-like drinking. They also showed direct evidence of axonal myelin damage in those brain regions as well as worse performance on a rat working memory task.

The fornix is a bundle of nerve fibers that connects subcortical and basal forebrain structures (including thalamus, nucleus accumbens) to the hippocampus (crus of the fornix). While microstructural deficits in REL were not identified in the central part of the fornix (the midline structure close to the subcortical nuclei), we detected both FA and MD deficits in the stria terminalis/fornix region, where fornix fibers in the parietal-temporal junction connect to the hippocampal formation; the lower FA in the right stria terminalis/fornix region of REL was related to longer smoking duration. The fornix is important for memory performance in the elderly (Oishi and Lyketsos, 2016 and references cited therein), and any potential injury may also affect any reduced memory performance observed in AUD (e.g., Durazzo et al., 2007). Furthermore, activity of the bed nucleus of the stria terminalis correlates with anxiety, acute stress and behavioral inhibition. Carrying fibers between the amygdala via thalamic areas to the orbitofrontal cortex, the stria terminalis and its function have also been linked to drug seeking behavior in rodents (Erb et al., 2001).

Taken together, microstructural injury to these prefrontal and limbic regions in REL may contribute to conditions that lead to relapse within 6–9 months after treatment initiation. Generally, the FA and MD

measures in these prefrontal and limbic regions did not correlate with measures of lifetime or recent substance use (alcohol and tobacco), consistent with previous reports (Sorg et al., 2012) and the possibility that the DTI abnormalities are premorbid. While we saw recovery of initially low FA values in most of these individuals between 1 and 4 weeks of abstinence into the range of healthy controls in corpus callosum, major frontocortico-striatal tracts and limbic pathways (Zou et al., 2017), these regions were not the same as those shown here to differentiate REL from ABST. Only more long-term longitudinal studies will allow testing for the possibility of premorbid effects of microstructural injury on treatment outcome.

Most alcohol-dependent individuals in North America are also chronic cigarette smokers (e.g., Gudyish et al., 2016). Cigarette smoking alone has detrimental effects on neurobiology and cognition (Bolego et al., 2002; Durazzo et al., 2010; Durazzo et al., 2014a; Durazzo et al., 2014b; Garey et al., 2004; Hawkins et al., 2002). Regarding microstructural morphology, chronic smoking has been associated with both lower and higher FA values within corpus callosum, anterior white matter and fronto-striatal fibers (Hudkins et al., 2015; Lin et al., 2013; Paul et al., 2008; Savjani et al., 2014; Yu et al., 2015; Zhang et al., 2011). The literature on the effects of chronic smoking on white matter microstructure in AUD is sparse: it shows no (Monnig et al., 2015) or only weak cross sectional effects and some evidence of greater short-term recovery from microstructural injury in non-smoking than smoking treatment seekers (Gazdzinski et al., 2010), with quite heterogeneous findings across individuals and regions in our more recent and larger longitudinal DTI study (Zou et al., 2017). While smoking status did not significantly affect microstructural differences between REL and ABST in our analyses, longer smoking duration in REL was associated moderately strong with lower FA in right stria terminalis/fornix, suggesting a localized microstructural effect of chronic smoking with functional relevance to relapse behavior. Potentially associated with effects on memory and drug seeking, this limbic structure may be involved in neural mechanisms by which smoking modulates, even hinders recovery from memory deficits in individuals with AUD (Durazzo et al., 2007). Therefore, smoking cessation during treatment for alcohol dependence may be a means to mitigate against even further microstructural decline in these fiber bundles and to improve outcome in AUD treatment.

The brain regions with microstructural abnormalities in this study (ABST vs. REL) were very similar to the regions in our previous study of longitudinal recovery from such abnormalities with abstinence (Zou et al., 2017) and there appeared to be no other major group differences outside our *a priori* specified ROIs and their contralateral regions (as shown by our secondary and exploratory analyses). Therefore, taken together, our findings suggest that white matter microstructure recovers in those who manage to maintain long-term abstinence and does not appear to recover as efficiently (or is premorbidly abnormal to some degree) in future relapsers; cigarette smoking exacerbates at least some regional microstructural injury.

This study has limitations: We studied treatment-seeking veterans who were mostly Caucasian and male; thus, our findings may not generalize to other AUD populations, and studying effects of gender and ethnicity was not possible. However, our main comparison groups were equivalent on behavioral, substance use and mood variables and major mental illness was exclusionary, assuring that the group differences pertained mostly to future treatment outcome. From an experimental point-of-view, diffusion was encoded in only six directions as we initiated the studies over ten years ago; this does allow TBSS analyses of major white matter tracts without the common problems of image misregistration, but not more detailed tractography. TBSS has several methodological challenges (Bach et al., 2014 and references cited therein): for example, the orientation information is discarded when ‘skeletonizing’ white matter tracts, so that anatomical connectivity between different brain regions cannot be analyzed, and merging or crossing fibers cannot be properly resolved, so that diffusion metrics

derived from the tensors in these regions do not properly represent the white matter microstructure. Free water can have partial volume averaging effects, which results in underestimation of the DTI metrics measured from some white matter tracts anatomically close to cerebrospinal fluid (e.g. the corpus callosum) (Jung, 2014). Finally, we did not explore axial and radial diffusivity, given cautionary statements in the literature on the interpretation of these measures in the case of crossing fibers (e.g., Wheeler-Kingshott and Cercignani, 2009).

Notwithstanding the specific limitations of this analysis, TBSS analyses of DTI data can provide valuable information on neurobiological correlates of relapse that can inform addiction treatment in the spirit of precision medicine. Specifically, such data contribute to the definition of a neurobiological relapse risk profile in AUD, which has clinical value for identifying individuals at greatest risk of relapse. Those treatment seekers at higher risk may benefit most from additional resources or extended follow-up to improve their long-term treatment outcomes.

Authors' contributions

DJM conceived, designed, and obtained funding for the study, oversaw data acquisition, processing, and analyses and edited the manuscript. YZ processed the MRI data, performed the statistical analyses, and drafted the manuscript. DEM acquired and processed some of the data and maintained the imaging database. TAM assisted with data processing. TPS recruited and assessed the study participants. TCD had intellectual input into the study design, trained YZ in statistical analyses, and helped conceptualize the data analyses. All authors contributed substantially to the content of the manuscript, critically reviewed the first draft and approved the final version for publication.

Acknowledgments

This investigation was supported by NIH AA10788 (DJM) and DA024136 (TCD) and by San Francisco VA Medical Center resources. The research was administered by the Northern California Institute for Research and Education. The funding and administrative agencies had no role in the design of the study, the collection and analysis of data or the decision to publish. We extend our appreciation to all who volunteered for this research. For critical help with participant recruitment and assessment, we thank the substance abuse treatment personnel at the San Francisco VA as well as Dr. David Pating and his team at Kaiser Permanente San Francisco.

Supplementary materials

Supplementary material associated with this article can be found, in the online version, at doi:10.1016/j.psychres.2018.09.004.

References

Bach, M., Laun, F.B., Leemans, A., Tax, C.M., Biessels, G.J., Stieltjes, B., et al., 2014. Methodological considerations on tract-based spatial statistics (TBSS). *Neuroimage* 100, 358–369.

Beaulieu, C., 2002. The basis of anisotropic water diffusion in the nervous system - a technical review. *NMR Biomed.* 15, 435–455.

Beck, A.T., 1978. *Depression Inventory*. Center for Cognitive Therapy, Philadelphia.

Beck, A., Wustenberg, T., Genauck, A., Wrase, J., Schlagenhauf, F., Smolka, M.N., et al., 2012. Effect of brain structure, brain function, and brain connectivity on relapse in alcohol-dependent patients. *Arch. Gen. Psychiatry* 69, 842–852.

Bolego, C., Poli, A., Paoletti, R., 2002. Smoking and gender. *Cardiovasc. Res.* 53, 568–576.

Bucur, B., Madden, D.J., Spaniol, J., Provenza, J.M., Cabeza, R., White, L.E., et al., 2008. Age-related slowing of memory retrieval: contributions of perceptual speed and cerebral white matter integrity. *Neurobiol. Aging* 29, 1070–1079.

Buhler, M., Mann, K., 2011. Alcohol and the human brain: a systematic review of different neuroimaging methods. *Alcohol Clin. Exp. Res.* 35, 1771–1793.

Cardenas, V.A., Durazzo, T.C., Gazdzinski, S., Mon, A., Studholme, C., Meyerhoff, D.J., 2011. Brain morphology at entry into treatment for alcohol dependence is related to relapse propensity. *Biol. Psychiatry* 70, 561–567.

Chung, T., Pajtek, S., Clark, D.B., 2013. White matter integrity as a link in the association between motivation to abstain and treatment outcome in adolescent substance users. *Psychol. Addict. Behav.* 27, 533–542.

Durazzo, T.C., Gazdzinski, S., Yeh, P.H., Meyerhoff, D.J., 2008. Combined neuroimaging, neurocognitive and psychiatric factors to predict alcohol consumption following treatment for alcohol dependence. *Alcohol Alcohol.* 43, 683–691.

Durazzo, T.C., Meyerhoff, D.J., Nixon, S.J., 2010. Chronic cigarette smoking: implications for neurocognition and brain neurobiology. *Int. J. Environ. Res. Public Health* 7, 3760–3791.

Durazzo, T.C., Mon, A., Pennington, D., Abe, C., Gazdzinski, S., Meyerhoff, D.J., 2014a. Interactive effects of chronic cigarette smoking and age on brain volumes in controls and alcohol-dependent individuals in early abstinence. *Addict. Biol.* 19, 132–143.

Durazzo, T.C., Pennington, D.L., Schmidt, T.P., Meyerhoff, D.J., 2014b. Effects of cigarette smoking history on neurocognitive recovery over 8 months of abstinence in alcohol-dependent individuals. *Alcohol Clin. Exp. Res.* 38, 2816–2825.

Durazzo, T.C., Rothlind, J.C., Gazdzinski, S., Banys, P., Meyerhoff, D.J., 2007. Chronic smoking is associated with differential neurocognitive recovery in abstinent alcoholic patients: a preliminary investigation. *Alcohol Clin. Exp. Res.* 31, 1114–1127.

Durazzo, T.C., Tosun, D., Buckley, S., Gazdzinski, S., Mon, A., Fryer, S.L., et al., 2011. Cortical thickness, surface area, and volume of the brain reward system in alcohol dependence: relationships to relapse and extended abstinence. *Alcohol Clin. Exp. Res.* 35, 1187–1200.

Erb, S., Salmaso, N., Rodaros, D., Stewart, J., 2001. A role for the CRF-containing pathway from central nucleus of the amygdala to bed nucleus of the stria terminalis in the stress-induced reinstatement of cocaine seeking in rats. *Psychopharmacology (Berl.)* 158, 360–365.

Fortier, C.B., Leritz, E.C., Salat, D.H., Lindemer, E., Maksimovskiy, A.L., Shepel, J., et al., 2014. Widespread effects of alcohol on white matter microstructure. *Alcohol Clin. Exp. Res.* 38, 2925–2933.

Gabrieli, J.D., Ghosh, S.S., Whitfield-Gabrieli, S., 2015. Prediction as a humanitarian and pragmatic contribution from human cognitive neuroscience. *Neuron* 85, 11–26.

Garey, K.W., Neuhauser, M.M., Robbins, R.A., Danziger, L.H., Rubinstein, I., 2004. Markers of inflammation in exhaled breath condensate of young healthy smokers. *Chest* 125, 22–26.

Gazdzinski, S., Durazzo, T.C., Mon, A., Yeh, P.H., Meyerhoff, D.J., 2010. Cerebral white matter recovery in abstinent alcoholics - a multimodal magnetic resonance study. *Brain (April)*, 1043–1053.

Grant, B.F., Goldstein, R.B., Saha, T.D., Chou, S.P., Jung, J., Zhang, H., et al., 2015. Epidemiology of DSM-5 alcohol use disorder: results from the national epidemiologic survey on alcohol and related conditions III. *JAMA Psychiatry* 72, 757–766.

Guydish, J., Passalacqua, E., Pagano, A., Martinez, C., Le, T., Chun, J., et al., 2016. An international systematic review of smoking prevalence in addiction treatment. *Addiction* 111, 220–230.

Hawkins, B.T., Brown, R.C., Davis, T.P., 2002. Smoking and ischemic stroke: a role for nicotine? *Trends Pharmacol. Sci.* 23, 78–82.

Heatherington, T.F., Kozlowski, L.T., Fracker, R.C., Fagerström, K.O., 1991. The Fagerström Test for Nicotine Dependence: a revision of the Fagerström Questionnaire. *Br. J. Addict.* 86, 1119–1127.

Hudkins, M., O'Neill, J., Tobias, M.C., Bartzokis, G., London, E.D., 2012. Cigarette smoking and white matter microstructure. *Psychopharmacology (Berl.)* 221, 285–295.

Jung, K.J., 2014. Removal of partial volume averaging with free water in MR diffusion tensor imaging using inversion recovery for b0 image. *Magn. Reson. Imaging* 32, 619–624.

Kirshenbaum, A.P., Olsen, D.M., Bickel, W.K., 2009. A quantitative review of the ubiquitous relapse curve. *J. Substance Abuse Treatment* 36, 8–17.

Koob, G.F., Volkow, N.D., 2016. Neurobiology of addiction: a neurocircuitry analysis. *Lancet Psychiatry* 3, 760–773.

Kuceyeski, A., Meyerhoff, D.J., Durazzo, T.C., Raj, A., 2013. Loss in connectivity among regions of the brain reward system in alcohol dependence. *Hum. Brain Mapp.* 34, 3129–3142.

Lebel, C., Gee, M., Camicioli, R., Wieler, M., Martin, W., Beaulieu, C., 2012. Diffusion tensor imaging of white matter tract evolution over the lifespan. *Neuroimage* 60, 340–352.

Lin, F., Wu, G., Zhu, L., Lei, H., 2013. Heavy smokers show abnormal microstructural integrity in the anterior corpus callosum: a diffusion tensor imaging study with tract-based spatial statistics. *Drug Alcohol Depend.* 129, 82–87.

Maisto, S.A., Clifford, P.R., Stout, R.L., Davis, C.M., 2006. Drinking in the year after treatment as a predictor of three-year drinking outcomes. *J. Stud. Alcohol* 67, 823–832.

Maisto, S.A., Clifford, P.R., Stout, R.L., Davis, C.M., 2007. Moderate drinking in the first year after treatment as a predictor of three-year outcomes. *J. Stud. Alcohol Drugs* 68, 419–427.

Mertens, J.R., Weisner, C., Ray, G.T., Fireman, B., Walsh, K., 2005. Hazardous drinkers and drug users in HMO primary care: prevalence, medical conditions, and costs. *Alcohol Clin. Exp. Res.* 29, 989–998.

Meyerhoff, D.J., Durazzo, T.C., 2010. Predicting relapse and treatment outcome in alcohol use disorders: Time for an integrative biopsychosocial approach. *Alcohol Clin. Exp. Res.* 34, 289A–290A.

Meyerhoff, D.J., Durazzo, T.C., Ende, G., 2013. Chronic alcohol consumption, abstinence and relapse: brain proton magnetic resonance spectroscopy studies in animals and humans. *Current Top. Behav. Neurosci.* 13, 511–540.

Moeller, S.J., Paulus, M.P., 2018. Toward biomarkers of the addicted human brain: Using neuroimaging to predict relapse and sustained abstinence in substance use disorder. *Prog. Neuropsychopharmacol. Biol. Psychiatry* 80, 143–154.

Monge, Z.A., Greenwood, P.M., Parasuraman, R., Strenziok, M., 2016. Individual

- differences in reasoning and visuospatial attention are associated with prefrontal and parietal white matter tracts in healthy older adults. *Neuropsychology* 30, 558–567.
- Monnig, M.A., Yeo, R.A., Tonigan, J.S., McCrady, B.S., Thoma, R.J., Sabbineni, A., et al., 2015. Associations of white matter microstructure with clinical and demographic characteristics in heavy drinkers. *PLoS One* 10, e0142042.
- Mori, S., Wakana, S., Nagae-Poetscher, L.M., Zijl, P.C.M.v., 2005. *MRI Atlas of Human White Matter*. Elsevier, Amsterdam.
- Müller-Oehring, E.M., Jung, Y.C., Pfefferbaum, A., Sullivan, E.V., Schulte, T., 2015. The resting brain of alcoholics. *Cereb. Cortex* 25, 4155–4168.
- Nichols, T.E., Holmes, A.P., 2002. Nonparametric permutation tests for functional neuroimaging: a primer with examples. *Hum. Brain Mapp.* 15, 1–25.
- Oishi, K., Lyketsos, C.G., 2016. Editorial: Alzheimer's disease and the fornix. *Front. Aging Neurosci.* 8, 149.
- Patton, J.H., Stanford, M.S., Barratt, E.S., 1995. Factor structure of the Barratt impulsiveness scale. *J. Clin. Psychol.* 51, 768–774.
- Pennington, D.L., Durazzo, T.C., Schmidt, T., Mon, A., Abe, C., Meyerhoff, D.J., 2013. The effects of chronic cigarette smoking on cognitive recovery during early abstinence from alcohol. *Alcohol Clin. Exp. Res.* 37, 1220–1227.
- Paul, R.H., Grieve, S.M., Niaura, R., David, S.P., Laidlaw, D.H., Cohen, R., et al., 2008. Chronic cigarette smoking and the microstructural integrity of white matter in healthy adults: a diffusion tensor imaging study. *Nicotine Tob. Res.* 10, 137–147.
- Peters, A., 2002. The effects of normal aging on myelin and nerve fibers: a review. *J. Neurocytol.* 31, 581–593.
- Pfefferbaum, A., Rosenbloom, M.J., Chu, W., Sassoon, S.A., Rohlfing, T., Pohl, K.M., et al., 2014. White matter microstructural recovery with abstinence and decline with relapse in alcohol dependence interacts with normal ageing: a controlled longitudinal DTI study. *Lancet Psychiatry* 1, 202–212.
- Pfefferbaum, A., Rosenbloom, M.J., Serventi, K.L., Sullivan, E.V., 2004. Brain volumes, RBC status, and hepatic function in alcoholics after 1 and 4 weeks of sobriety: predictors of outcome. *Am. J. Psychiatry* 161, 1190–1196.
- Rando, K., Hong, K.I., Bhagwagar, Z., Li, C.S., Bergquist, K., Guarnaccia, J., et al., 2011. Association of frontal and posterior cortical gray matter volume with time to alcohol relapse: a prospective study. *Am. J. Psychiatry* 168, 183–192.
- Reitan, R.M., Wolfson, D., 1985. *The Halstead-Reitan Neuropsychological Test Battery: Theory and Interpretation*. AZ: Neuropsychological Press, Tucson.
- Savjani, R.R., Velasquez, K.M., Thompson-Lake, D.G., Baldwin, P.R., Eagleman, D.M., De La Garza 2nd, R., Salas, R., 2014. Characterizing white matter changes in cigarette smokers via diffusion tensor imaging. *Drug Alcohol Depend.* 145, 134–142.
- Schulte, T., Sullivan, E.V., Muller-Oehring, E.M., Adalsteinsson, E., Pfefferbaum, A., 2005. Corpus callosal microstructural integrity influences interhemispheric processing: a diffusion tensor imaging study. *Cereb. Cortex* 15, 1384–1392.
- Seo, D., Sinha, R., 2014. The neurobiology of alcohol craving and relapse. *Handbook of Clinical Neurology* 125, pp. 355–368.
- Seo, D., Sinha, R., 2015. Neuroplasticity and predictors of alcohol recovery. *Alcohol Res.* 37, 143–152.
- Seo, S., Mohr, J., Beck, A., Wustenberg, T., Heinz, A., Obermayer, K., 2015. Predicting the future relapse of alcohol-dependent patients from structural and functional brain images. *Addict. Biol.* 20, 1042–1055.
- Smith, S.M., Jenkinson, M., Johansen-Berg, H., Rueckert, D., Nichols, T.E., Mackay, C.E., et al., 2006. Tract-based spatial statistics: voxelwise analysis of multi-subject diffusion data. *Neuroimage* 31, 1487–1505.
- Sorg, S.F., Squeglia, L.M., Taylor, M.J., Alhassoon, O.M., Delano-Wood, L.M., Grant, I., 2015. Effects of aging on frontal white matter microstructure in alcohol use disorder and associations with processing speed. *J. Stud. Alcohol Drugs* 76, 296–306.
- Sorg, S.F., Taylor, M.J., Alhassoon, O.M., Gongvatana, A., Theilmann, R.J., Frank, L.R., et al., 2012. Frontal white matter integrity predictors of adult alcohol treatment outcome. *Biol. Psychiatry* 71, 262–268.
- Spielberger, C.D., Gorsuch, R.L., Lushene, R., Vagg, P.R., Jacobs, G.A., 1977. *Self-Evaluation Questionnaire*.
- Van Leemput, K., Maes, F., Vandermeulen, D., Suetens, P., 1999a. Automated model-based bias field correction of MR images of the brain. *IEEE Trans. Med. Imaging* 18, 885–896.
- Van Leemput, K., Maes, F., Vandermeulen, D., Suetens, P., 1999b. Automated model-based tissue classification of MR images of the brain. *IEEE Trans. Med. Imaging* 18, 897–908.
- Vargas, W.M., Bengston, L., Gilpin, N.W., Whitcomb, B.W., Richardson, H.N., 2014. Alcohol binge drinking during adolescence or dependence during adulthood reduces prefrontal myelin in male rats. *J. Neurosci.* 34, 14777–14782.
- Volkow, N.D., Baler, R.D., 2013. Brain imaging biomarkers to predict relapse in alcohol addiction. *JAMA Psychiatry* 70, 661–663.
- Volkow, N.D., Wang, G.J., Fowler, J.S., Tomasi, D., 2012. Addiction circuitry in the human brain. *Annu. Rev. Pharmacol. Toxicol.* 52, 321–336.
- Wechsler, D., 1997. *The Wechsler Adult Intelligence Scale*, third ed. The Psychological Corporation, San Antonio, TX.
- Weinberger, A.H., Platt, J., Jiang, B., Goodwin, R.D., 2015. Cigarette smoking and risk of alcohol use relapse among adults in recovery from alcohol use disorders. *Alcohol Clin. Exp. Res.* 39, 1989–1996.
- Wheeler-Kingshott, C.A., Cercignani, M., 2009. About "axial" and "radial" diffusivities. *Magn. Reson. Med.* 61, 1255–1260.
- Witkiewitz, K., 2011. Predictors of heavy drinking during and following treatment. *Psychol. Addict. Behav.* 25, 426–438.
- Witkiewitz, K., Marlatt, G.A., 2007. Modeling the complexity of post-treatment drinking: it's a rocky road to relapse. *Clin. Psychol. Rev.* 27, 724–738.
- Wrase, J., Makris, N., Braus, D.F., Mann, K., Smolka, M.N., Kennedy, D.N., et al., 2008. Amygdala volume associated with alcohol abuse relapse and craving. *Am. J. Psychiatry* 165, 1179–1184.
- Xiao, P., Dai, Z., Zhong, J., Zhu, Y., Shi, H., Pan, P., 2015. Regional gray matter deficits in alcohol dependence: a meta-analysis of voxel-based morphometry studies. *Drug Alcohol Depend.* 153, 22–28.
- Yeh, P.H., Simpson, K., Durazzo, T.C., Gazdzinski, S., Meyerhoff, D.J., 2008. Tract-based spatial statistics (TBSS) of diffusion tensor imaging data in alcohol dependence: abnormalities of the motivational neurocircuitry. *Psychiatry Res.* 173, 22–30.
- Yu, D., Yuan, K., Zhang, B., Liu, J., Dong, M., Jin, C., et al., 2015. White matter integrity in young smokers: a tract-based spatial statistics study. *Addict. Biol.* 21, 679–687.
- Zahr, N.M., 2014. Structural and microstructural imaging of the brain in alcohol use disorders. *Handbook of Clinical Neurology* 125, pp. 275–290.
- Zhang, X., Salmeron, B.J., Ross, T.J., Geng, X., Yang, Y., Stein, E.A., 2011. Factors underlying prefrontal and insula structural alterations in smokers. *Neuroimage* 54, 42–44.
- Zou, Y., Murray, D.E., Durazzo, T.C., Schmidt, T.P., Murray, T.A., Meyerhoff, D.J., 2017. Effects of abstinence and chronic cigarette smoking on white matter microstructure in alcohol dependence: diffusion tensor imaging at 4T. *Drug Alcohol Depend.* 175, 42–50.